AN EXTENSION OF THE MODIFIED ELEMENT FREE GALERKIN METHOD APPLIED TO LARGE DEFORMATION PROBLEMS

Rodrigo Rossi
Dep. Mechanical Eng., Universidade de Caxias do Sul, *Bloco D*, Caxias do Sul, RS, 95070-560, Brazil
rrossi@ucs.br

Marcelo Krajnc Alves
Dep. Mechanical Eng., Universidade Federal de Santa Catarina, Florianópolis, SC, 88010-970, Brazil
krajnc@emc.ufsc.br

Hazim Ali Al-Qureshi
Dep. Mechanical Eng., Universidade Federal de Santa Catarina, Florianópolis, SC, 88010-970, Brazil
hazim@materiais.ufsc.br

Abstract. *In this work we investigate a modified element-free Galerkin method when applied to a large deformation process. The modified element-free Galerkin method presented in this work enables the direct imposition of the essential boundary conditions due to the kronecker delta property of special shape functions constructed in the neighborhood of the essential boundary. The model assumes the multiplicative decomposition of the deformation gradient into elastic and plastic parts and considers a J_2 elasto-plastic constitutive relationship with a nonlinear isotropic hardening. The constitutive model is written in terms of the rotated Kirchoff stress and the logarithmic strain conjugate measure. A Total Lagrangian formulation is considered. Some numerical results are presented, under axisymmetric assumption, in order to attest the performance of the proposed methodology. Some aspects related to volumetric locking are investigated by considering an F-bar method.*

Keywords*: Large deformations, Mesh-free, Volumetric locking.*

1. Introduction

In this work the MEFG proposed in Alves and Rossi (2003) will be numerically investigated when applied to large deformation problems. More specifically, the proposed procedure considers: a *Total Lagrangian* description; a multiplicative decomposition of the deformation gradient, into plastic and elastic parts, and a constitutive equations, given in terms of the logarithmic deformation measure and the rotated *Kirchoff* stress. In this model the stress response is assumed to be hyperelastic.

The use of the rotated *Kirchoff* stress together with the logarithmic deformation measure, ln(**U**), was first described in Eterovic and Bathe (1990) and Weber and Anand (1990) and was also studied by others authors, as Akkaram and Zabaras (2001). Similar investigations are also presented in Souza Neto *et al.* (2002) and Souza Neto *et al.* (1996) where, however, an *Eulerian* description is adopted based on the *Kirchoff* stress and the logarithmic deformation measure, ln(**V**).

The J_2 plasticity model presented in this work assumes the hypothesis of incompressibility of the plastic flow. This hypothesis leads to the so called volumetric locking phenomenon, which occurs if one uses, for instance, a low order finite element approximation when solving plane strains and axisymmetric problems. Such phenomenon is also verified in mesh-free methods as mention in Askes *et al.* (1999) and Huerta and Méndez (2001).

The *B-bar* method ($\overline{\mathbf{B}}$) proposed by Hughes (1980), the enhanced assumed strain method (EAS) proposed by Simo, and Rifai (1990) and the known as *F-bar* method ($\overline{\mathbf{F}}$) proposed by Souza Neto *et al.* (1996) are examples of methodologies largely used in the literature in order to circumvent volume locking phenomena, when using low order finite elements. These methodologies are formulated in a general frame work and may be applied, without significant changes, to the MEFG method.

More specifically on the volumetric locking phenomena in EFG methods, some procedures were proposed in order to overcome it. Wells *et al.* (2002) propose that a local extrinsic enrichment be accomplished just where the plastic flow takes place. In Askes *et al.* (1999), it is numerically shown, for near incompressible solids, that the volumetric locking problem is not evidenced if a sufficiently large support of the global shape function is used. However, Huerta and Méndez (2001) shows that the volumetric locking problem is just attenuated, but not suppressed from the analysis. Mixed formulations, where the displacements and pressure fields are approximated separately, are also proposed in the literature in the context of mesh-free methods together with strategies of selective integration. In this case the inf sup condition of *Ladyzhenskaya-Brezi-Babuska* (LBB) must be satisfied.

In this work an *F-bar* method ($\overline{\mathbf{F}}$) is implemented and investigated under axisymmetric conditions. Such choice is due to the simplicity of implementation of the method, when compared with the other methods, and for the good results obtained by Souza Neto *et al.* (1996), Souza Neto *et al.* (2002) and Akkaram and Zabaras (2001).

2. A brief description of the modified element-free galerkin method

• **Moving least square approximation:** By the use of a MLSA it is possible to construct an approximation function $u^h(\boldsymbol{X})$ that fits a discrete set of data $\{u_I, I=1\ldots n\}$ such that:

$$u^h(\boldsymbol{X}) = \sum_{I=1}^{n} \Phi_I(\boldsymbol{X}) u_I \,, \tag{1}$$

$$\Phi_I(\boldsymbol{X}) = \boldsymbol{p}(\boldsymbol{X}) \cdot \mathbf{A}(\boldsymbol{X})^{-1} \boldsymbol{b}_I(\boldsymbol{X}) \tag{2}$$

$$\mathbf{A}(\boldsymbol{X}) = \sum_{I=1}^{n} w(\boldsymbol{X} - \boldsymbol{X}_I)\left[\boldsymbol{p}(\boldsymbol{X}_I) \otimes \boldsymbol{p}(\boldsymbol{X}_I)\right] \text{ and } \mathbf{b}_I(\boldsymbol{X}) = w(\boldsymbol{X} - \boldsymbol{X}_I)\mathbf{p}(\boldsymbol{X}_I), \tag{3}$$

where $\{p_j(\boldsymbol{X}), j=1\ldots m\}$ represents the set of intrinsic base functions and $w(\boldsymbol{X} - \boldsymbol{X}_I)$ is a weight function centered at $\boldsymbol{X}_I$. Here, $\Phi_I(\boldsymbol{X})$ is the global shape function, defined at particle $\boldsymbol{X}_I$, and $\mathbf{A}(\boldsymbol{X})$ is the moment matrix.

• **Element-free Galerkin:** The conventional EFG method is characterized by the construction of a set of global shape functions, $\Phi_I(\boldsymbol{X})$ defined at particle $\boldsymbol{X}_I$, which defines the approximation space, used by the Galerkin method to solve a boundary value problem. The particle distribution that defines how the covering of the domain is performed, by the global shape functions $\Phi_I(\boldsymbol{X})$, is not arbitrary since it must satisfy the stability condition

$$card\left\{\boldsymbol{X}_J \,|\, \Phi_J(\boldsymbol{X}) \neq 0\right\} \geq \dim\left[\mathbf{A}(\boldsymbol{X})\right] \tag{4}$$

i.e., the number of particles $\boldsymbol{X}_J$ whose associated shape function $\Phi_J(\boldsymbol{X})$ have a nonzero value at $\boldsymbol{X}$, must be larger that the size of $\mathbf{A}(\boldsymbol{X})$, which is given by the number of intrinsic base functions in $\boldsymbol{p}(\boldsymbol{X})$. Moreover, for $\boldsymbol{X} \in R^n$, there must be $n+1$ particles, whose position vectors form a nonzero n-th rank simplex element, 0. In order to obtain a particle distribution that comply with Eq.(4), we perform a partition of the domain, Ω, into a triangular integration mesh, where we consider each triangular partition/element to be an integration cell and each vertex node to be the position of a particle.

One of the most common weight function is the quartic-spline function, w^{EFG}, given as:

$$w^{EFG}(r) = \begin{cases} 1 - 6r^2 + 8r^3 - 3r^4, & \text{for } r \leq 1.0 \\ 0, & \text{for } r > 1.0 \end{cases} \tag{5}$$

where $r = r_I / \overline{r}_I$ with $r_I = \left\| \boldsymbol{X} - \boldsymbol{X}_I \right\|$. The radius $\overline{r}_I$, defining the support of $w^{EFG}(\boldsymbol{X} - \boldsymbol{X}_I)$, is determined by

$$\overline{r}_I = \beta \cdot r_{I\max}, \qquad \beta > 1, \;\; \beta \in R \text{ with } r_{I\max} = \max_i \left\| \boldsymbol{X}_i - \boldsymbol{X}_I \right\|, \quad i \in J_I \,, \tag{6}$$

where J_I represents the set of adjacent nodes associated with $\boldsymbol{x}_I$.

Now, in the conventional EFG method, the global shape functions $\{\Phi_I(\boldsymbol{X}), I=1\ldots n\}$, defining the approximation space, do not satisfy, in general, the kronecker delta property, i.e., $\Phi_I(\boldsymbol{X}_J) \neq \delta_{IJ}$. As a consequence, it is not possible to enforce the essential boundary conditions, by directly prescribing nodal values, as done in the FEM. However, special weight functions may be constructed in order to satisfy the kronecker delta property. Among the possible weight functions is the extended partition of unity finite element (EPUFE) weight function.

• **Extended Partition of unity finite element weight functions:** The global shape functions $\{\Phi_I(\boldsymbol{X}), I=1\ldots n\}$, employed in EPUFE, are obtained by a MLSA. A typical support of an EPUFE global shape function is illustrated in Figure 2, where one can identify the adjacent extended node list of $\boldsymbol{X}_I$ given by the set $\{\boldsymbol{X}_1^*, \boldsymbol{X}_2^*, \boldsymbol{X}_3^* \; \boldsymbol{X}_4^* \; \boldsymbol{X}_5^*\}$. Now, in the case where a linear triangular finite element base function is used as a weight function for the MLSA, one derives:

$$w^{EPF}\left(\boldsymbol{X}^* - \boldsymbol{X}_I\right) = \begin{cases} \frac{1}{2A}\left[\left(x_i^* y_{i+1}^* - x_{i+1}^* y_i^*\right) + \left(y_i^* - y_{i+1}^*\right)x + \left(x_{i+1}^* - x_i^*\right)y\right], & \boldsymbol{X} \in \text{supp}\left[\Phi_I(\boldsymbol{X})\right] \\ 0, \;\; \text{otherwise} \end{cases} \tag{7}$$

Here, $\boldsymbol{X}_i^*$ and $\boldsymbol{X}_{i+1}^*$ are the elements of the adjacent extended node list set of $\boldsymbol{X}_I$, obtained in a counter clockwise sense of the triangular integration cell whose area is A. The usage of an intrinsic base $\boldsymbol{p}^T(\boldsymbol{X}) = [1, x, y]$ together with a

EPUFE weight function satisfy the requirement explicated in Eq.(4), therefore, this extension ensures the regularity of $\mathbf{A}(\boldsymbol{X})$.

The extended points are determined as: $\boldsymbol{X}_i^* = \boldsymbol{X}_i + \varepsilon\left(\boldsymbol{X}_i - \boldsymbol{X}_I\right)$. Notice that, letting $\varepsilon \to 0$, we derive a global shape function that satisfy, in a limiting sense, at a given particle $\boldsymbol{X}_J$, the kronecker delta property, i.e., $\lim_{\varepsilon \to 0} \Phi_I\left(\boldsymbol{X}_J\right) = \delta_{IJ}$.

• **Modified element-free Galerkin method:** The objective of the MEFG method is to combine, in a suitable way, both weight functions, in order to explore the smoothness of w^{EFG} and the kronecker delta property of w^{EPF}. The strategy can be shown by considering a body with domain Ω and boundary $\partial\Omega$, where $\partial\Omega = \Gamma_u \cup \Gamma_t$ and $\Gamma_u \cap \Gamma_t = \varnothing$. Here, Γ_u and Γ_t are respectively the part of $\partial\Omega$ with prescribed essential and natural boundary conditions, as illustrated in Figure 1. Notice that the EPUFE weight functions are specified at particles that belong to a neighborhood of Γ_u and the EFG weight functions are specified at the remaining particles of the mesh. This procedure enables the determination of an approximate solution that satisfies accurately the essential boundary condition and is smooth in the entire domain, except for a neighborhood of Γ_u. The MEFG method can be seen as a conventional EFG method, having a set of different weight functions, which is able to automatically select, at each particle, the proper type of weight function and to compute the adequate size of its support.

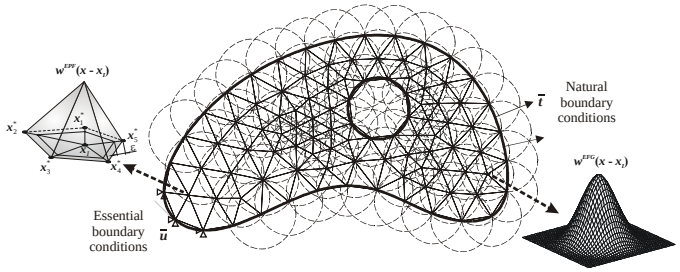

Fig. 1 An example of body coverage by the MEFG

Notice that, since the global shape functions are constructed with the same intrinsic base, the approximation keeps the reproducibility property over the entire domain, an important MLSA property. A sensitivity and convergence examination of the approximate solution with respect to the parameter ε is given in Alves and Rossi (2001).

3. Finite deformation

• **Kinematics of deformation:** The model presented in this paper considers the multiplicative decomposition of the deformation gradient $\mathbf{F}$ into an elastic, $\mathbf{F}^e$, and plastic parts, $\mathbf{F}^p$, so that $\mathbf{F} = \mathbf{F}^e\mathbf{F}^p$, with $\mathbf{F} = \nabla_{\boldsymbol{X}}\boldsymbol{\varphi}\left(\boldsymbol{X},t\right)$, see Figure 2.

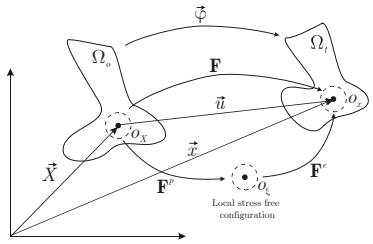

Fig. 2 Multiplicative decomposition of the deformation gradient.

Based in this assumption the rate of deformation can be decomposed additively as $\mathbf{D} = \mathbf{D}^e + \mathbf{D}^p$. The consideration of a J_2 plasticity model leads to $\det(\mathbf{F}^p) = 1$ and, since $\det(\mathbf{F}) > 0$, to $\det(\mathbf{F}^e) > 0$. Thus, the elastic deformation gradient admits a polar decomposition, i.e., $\mathbf{F}^e = \mathbf{R}^e\mathbf{U}^e$ where $\mathbf{U}^e = \sqrt{\mathbf{C}^e}$, $\mathbf{C}^e = \left(\mathbf{F}^e\right)^T\mathbf{F}^e$ and $\mathbf{R}^e$ is the elastic rotation tensor. Here, the elastic strain measure is the logarithmic or *Hencky* strain tensor given by $\mathbf{E}^e = \ln\left(\mathbf{U}^e\right)$ Now, as pointed by Hill (1978), and following Eterovic and Bathe (1990) and Weber and Anand (1990), in the formulation of constitutive theories, the stress-strain pairs must be such that the rate of work density remains preserved. Thus, the conjugate stress associated with the *Hencky* strain is the *rotated Kirchoff* stress $\bar{\mathbf{T}}$, given by $\bar{\mathbf{T}} = \left(\mathbf{R}^e\right)^T\boldsymbol{\tau}\mathbf{R}^e$.

• **Constitutive hyperelastic law, free energy and dissipation potentials:** The model investigated here considers a nonlinear isotropic hardening. The free energy potential is assumed to be given by

$$\rho_o \psi\left(\mathbf{E}^e, \alpha\right) = \frac{1}{2}\mathbb{D}\mathbf{E}^e \cdot \mathbf{E}^e + \frac{1}{2}H\alpha^2 + \left(\sigma_\infty - \sigma_y\right)\left[\alpha + \frac{1}{\delta}e^{-\delta\alpha}\right]. \tag{8}$$

where α is the isotropic hardening strain, ρ_o is the mass density, and H, δ, σ_∞ and σ_y are material parameters. $\mathbb{D}$ is the standard elasticity tensor, given as $\mathbb{D} = 2\mu\mathbb{I} + \left(\kappa - \frac{2}{3}\mu\right)\mathbf{I}\otimes\mathbf{I}$, with $\mathbb{I}$ and $\mathbf{I}$ being respectively the fourth order and the second order identities and μ and κ elastic material parameters known as shear and bulk modulus.

The state equations are given by

$$\bar{\mathbf{T}} = \rho_o \frac{\partial \psi\left(\mathbf{E}^e, \alpha\right)}{\partial \mathbf{E}^e} = \mathbb{D}\mathbf{E}^e \text{ and } k = \rho_o \frac{\partial \psi\left(\mathbf{E}^e, \alpha\right)}{\partial \alpha} = H\alpha + \left(\sigma_\infty - \sigma_y\right)\left(1 - e^{-\delta\alpha}\right). \tag{9}$$

Here, k is the isotropic hardening stress. This isotropic hardening relation was used in Simo and Armero (1992) and Souza Neto *et al.* (2002) where an investigation of the volumetric locking, in a large deformation process, was performed.

The dissipation is given by $D = \bar{\mathbf{T}} \cdot \bar{\mathbf{D}}^p + k \cdot \dot{\alpha} \geq 0$, where $\bar{\mathbf{D}}^p$ is the modified plastic stretching. Since the elasto-plastic model is assumed to be associative, the potential of dissipation $\mathcal{F}$ is given by the indicator function of the admissible stress space $\mathcal{E}$, $\mathcal{E} = \left\{\bar{\mathbf{T}} \,\middle|\, \mathcal{F}\left(\bar{\mathbf{T}}, k\right) \leq 0\right\}$, where the yield function is given by

$$\mathcal{F}\left(\bar{\mathbf{T}}, k\right) = \sqrt{3J_2} - \left[k\left(\alpha\right) + \sigma_y\right] \text{ with } J_2 = \frac{1}{2}\bar{\mathbf{T}}^D \cdot \bar{\mathbf{T}}^D \quad \text{and} \quad \bar{\mathbf{T}}^D = \bar{\mathbf{T}} - \frac{1}{3}\mathrm{tr}\left(\bar{\mathbf{T}}\right)\mathbf{I}. \tag{10}$$

By applying the normal dissipation hypothesis, we derive the plastic and hardening evolution laws, given by

$$\bar{\mathbf{D}}^p = \dot{\lambda}\frac{\partial \mathcal{F}}{\partial \bar{\mathbf{T}}} \text{ and } \dot{\alpha} = -\dot{\lambda}\frac{\partial \mathcal{F}}{\partial k}. \tag{11}$$

where $\dot{\lambda}$ is the plastic multiplier and must satisfy: $\mathcal{F} \leq 0$, $\dot{\lambda} \geq 0$ and $\dot{\lambda}\mathcal{F} = 0$.

4. Elasto-plastic initial value problem

The elasto-plastic problem presented in the previous section is dependent of the deformation history. Thus, in order to integrate the evolution equations from time step t_n to t_{n+1}, we must solve an initial value problem. The elasto-plastic initial value problem can be stated as, given the deformation history $\mathbf{F}(t), t \in [t_n, t_{n+1}]$, $\mathbf{F}^p\left(t_n\right) = \mathbf{F}_n^p$ and $\alpha\left(t_n\right) = \alpha_n$: determine $\mathbf{F}_{n+1}^p$ and α_{n+1} such that the Eq.(10), Eq.(11) and Eq.(9) are satisfied. The strategy employed in the solution of the nonlinear problem comprises two basic steps that are: an *elastic predictor* and a *plastic corrector*.

• **Elastic predictor:** The solution is initially assumed as purely hyperelastic and a *trial elastic state* is computed by

$$\mathbf{F}_{n+1}^{e^{trial}} = \mathbf{F}_{n+1}\left(\mathbf{F}_n^p\right)^{-1} \quad \mathbf{C}_{n+1}^{e^{trial}} = \left(\mathbf{F}_{n+1}^{e^{trial}}\right)^T \mathbf{F}_{n+1}^{e^{trial}} \quad \mathbf{E}_{n+1}^{e^{trial}} = \frac{1}{2}\ln\left(\mathbf{C}_{n+1}^{e^{trial}}\right) \quad \bar{\mathbf{T}}_{n+1}^{trial} = \mathbb{D}\mathbf{E}_{n+1}^{e^{trial}} \text{ and } k_{n+1}^{trial} = k_n \tag{12}$$

• **Plastic corrector:** The plastic corrector phase considers a *return mapping* algorithm that is obtained by the *backward exponential approximation* proposed in Eterovic and Bathe (1990), Weber and Anand (1990). This phase considers:

a. *The Verification of the yield function feasibility:* The plastic corrector is done only if $\bar{\mathbf{T}}_{n+1}^{trial} \notin \bar{\mathcal{E}}$, i.e., $\mathcal{F}\left(\bar{\mathbf{T}}_{n+1}^{trial}, k_{n+1}^{trial}\right) > 0$

b. *The performance of the Plastic correction:* At this point the evolution laws are discretized. The plastic evolution $\dot{\mathbf{F}}^p = \bar{\mathbf{D}}^p \mathbf{F}^p$ is discretized based on the *backward exponential approximation* resulting in $\mathbf{F}^p_{n+1} = \exp\left(\bar{\mathbf{D}}^p_{n+1}\right)\mathbf{F}^p_n$, which reduces to

$$\mathbf{E}^e_{n+1} = \mathbf{E}^{e^{trial}}_{n+1} - \Delta\lambda \mathbf{N}_{n+1} \text{ with } \mathbf{N}_{n+1} = \left.\frac{\partial \mathcal{F}}{\partial \bar{\mathbf{T}}}\right|_{n+1} \quad , \quad \bar{\mathbf{D}}^p_{n+1} = \Delta\lambda \mathbf{N}_{n+1} \text{ and } \mathbf{R}^e_{n+1} = \mathbf{R}^{e^{trial}}_{n+1} \tag{13}$$

The discretized form of the remaining evolution equations is performed by a standard *backward Euler method.* Summarizing, the solution of plastic corrector phase is obtained by solving Eq.(14), for $\mathbf{E}^e_{n+1}$, α_{n+1} and $\Delta\lambda$. Figure 3 sketches the deformation process in the algorithm.

$$\begin{cases} \mathbf{E}^e_{n+1} - \mathbf{E}^{e^{trial}}_{n+1} + \Delta\lambda \mathbf{N}_{n+1} \\ \alpha_{n+1} - \alpha_n - \Delta\lambda \\ \mathcal{F}\left(\bar{\mathbf{T}}_{n+1}, k\left(\alpha_{n+1}\right)\right) \end{cases} = \begin{bmatrix} 0 \\ 0 \\ 0 \end{bmatrix} \tag{14}$$

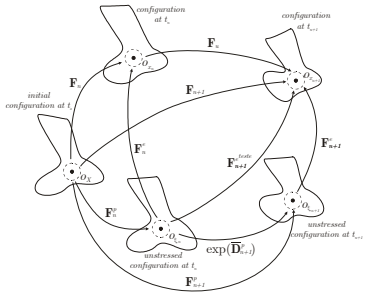

Fig. 3 Kinematics of deformation in the presented algorithm

5. Total Lagrangean formulation

• **Strong formulation:** The problem can be enounced as: Determine $\boldsymbol{u}$ such that

$$\begin{aligned} &\operatorname{div}\mathbf{P} - \rho_o \boldsymbol{b} = \boldsymbol{0} \quad \text{in } \Omega_o \\ &\mathbf{P}\boldsymbol{m} = \boldsymbol{t} \quad \text{in } \Gamma_t \quad \text{and} \quad \boldsymbol{u} = \bar{\boldsymbol{u}} \quad \text{in } \Gamma_u \end{aligned} \tag{15}$$

where $\mathbf{P}$ is the first *Piola-Kirchoff* stress, $\boldsymbol{b}$ is the body force vector, $\boldsymbol{m}$ is the outer normal on $\partial\Omega_o$, $\boldsymbol{t}$ is traction vector and $\bar{\boldsymbol{u}}$ is the prescribed displacement.

• **Weak form:** Here, the problem, in an incremental form, is posed as: Determine $\boldsymbol{u}_{n+1} \in H$, $H = \left\{\boldsymbol{u} \middle| u_i \in W^1_p(\Omega),\ \boldsymbol{u} = \bar{\boldsymbol{u}} \text{ on } \Gamma_u\right\}$, such that

$$\int_{\Omega_o} \mathbf{P}\left(\boldsymbol{u}_{n+1}\right) \cdot \nabla_{\boldsymbol{X}} \hat{\boldsymbol{u}}\, d\Omega_o - \int_{\Omega_o} \rho_o \boldsymbol{b} \cdot \hat{\boldsymbol{u}}\, d\Omega_o - \int_{\Gamma_{o_t}} \boldsymbol{t} \cdot \hat{\boldsymbol{u}}\, d\Gamma_{o_t} = 0 \quad \forall \hat{\boldsymbol{u}} \in H_o \tag{16}$$

• **Linearization and Newton method:** The solution of the nonlinear problem in Eq.(16) is achieved through a standard *Newton-Raphson* iteration method. In this context the linearization of the functional $\mathcal{G}\left(\boldsymbol{u}_{n+1}, \hat{\boldsymbol{u}}\right)$ is required. Here,

$$D\mathcal{G}\left(\boldsymbol{u}^k_{n+1}, \hat{\boldsymbol{u}}\right)\left[\Delta\boldsymbol{u}^k_{n+1}\right] = \int_{\Omega_o} \left[\mathbb{A}\left(\boldsymbol{u}_{n+1}\right)\right] \nabla_{\boldsymbol{X}}\left(\Delta\boldsymbol{u}^k_{n+1}\right) \cdot \nabla_{\boldsymbol{X}} \hat{\boldsymbol{u}}\, d\Omega_o \quad \text{with } [\mathbb{A}]_{ijkl} = \frac{\partial \tau_{ip}}{\partial F_{kl}} F^{-1}_{jp} - \tau_{ip} F^{-1}_{jk} F^{-1}_{lp}. \tag{17}$$

• **Determination of** $\mathbb{A}$: The determination of $\mathbb{A}$ requires the derivative of the *Kirchoff* stress tensor with respect to the deformation gradient. Now, the *Kirchoff* stress is related to the *rotated Kirchoff* stress. This means that in the determination of Eq.(17) a derivative of the *rotated Kirchoff* stress with respect to the deformation gradient takes place. But as $\overline{\mathbf{T}}_{n+1} = \hat{\overline{\mathbf{T}}}_{n+1}\left(\mathbf{E}^{e^{trial}}_{n+1}, (\bullet)_n\right)$, by using the chain rule of differentiation, we derive

$$\hat{\mathbb{D}} = \frac{\partial \overline{\mathbf{T}}_{n+1}}{\partial \mathbf{F}_{n+1}} = \frac{\partial \overline{\mathbf{T}}_{n+1}}{\partial \mathbf{E}^{e^{trial}}_{n+1}} \frac{\partial \mathbf{E}^{e^{trial}}_{n+1}}{\partial \mathbf{C}^{e^{trial}}_{n+1}} \frac{\partial \mathbf{C}^{e^{trial}}_{n+1}}{\partial \mathbf{F}_{n+1}} = \tilde{\mathbb{D}}\mathbb{G}\mathbb{H} \quad \text{where} \quad \tilde{\mathbb{D}} = \frac{\partial \overline{\mathbf{T}}_{n+1}}{\partial \mathbf{E}^{e^{trial}}_{n+1}},\ \mathbb{G} = \frac{\partial \mathbf{E}^{e^{trial}}_{n+1}}{\partial \mathbf{C}^{e^{trial}}_{n+1}} \quad \text{and} \quad \mathbb{H} = \frac{\partial \mathbf{C}^{e^{trial}}_{n+1}}{\partial \mathbf{F}_{n+1}}. \tag{18}$$

The terms $\mathbb{G}$ and $\mathbb{H}$ in Eq.(18) are related with the geometric part of $\hat{\mathbb{D}}$ and are determined by

$$[\mathbb{H}]_{ijkl} = \frac{\partial C^{e^{trial}}_{n+1_{ij}}}{\partial F_{n+1_{kl}}} = F^{p^{-1}}_{n_{li}} F^{e^{trial}}_{n+1_{kj}} + F^{e^{trial}}_{n+1_{ki}} F^{p^{-1}}_{n_{lj}} \quad \text{and} \quad \mathbb{G} = \frac{\partial \mathbf{E}^{e^{trial}}_{n+1}}{\partial \mathbf{C}^{e^{trial}}_{n+1}} = \frac{\partial}{\partial \mathbf{C}^{e^{trial}}_{n+1}} \ln\left(\mathbf{U}^{e^{trial}}_{n+1}\right) = \frac{1}{2} \frac{\partial}{\partial \mathbf{C}^{e^{trial}}_{n+1}} \ln\left(\mathbf{C}^{e^{trial}}_{n+1}\right). \tag{19}$$

Notice that $\tilde{\mathbb{D}}$ is the only contribution related to the constitutive relation in the consistent tangent modulus $\mathbb{A}$. Now, the determination depends if the state is elastic, $\mathcal{F} \leq 0$, or elasto-plastic $\mathcal{F} > 0$. Hence, $\tilde{\mathbb{D}} = \mathbb{D}$ if $\mathcal{F} \leq 0$ or $\tilde{\mathbb{D}} = \mathbb{D}^{ep}$ if $\mathcal{F} > 0$. Here, $\mathbb{D}^{ep}$ is the elasto-plastic modulus, which is given by

$$\mathbb{D}^{ep} = \frac{d\overline{\mathbf{T}}_{n+1}}{d\mathbf{E}^{e^{trial}}_{n+1}} = \left(\mathbb{D}^{-1} + \Delta\lambda \frac{\partial \mathbf{N}_{n+1}}{\partial \overline{\mathbf{T}}_{n+1}} - \frac{1}{\frac{\partial \mathcal{F}}{\partial \alpha_{n+1}}} \mathbf{N}_{n+1} \otimes \mathbf{N}_{n+1} \right)^{-1}. \tag{20}$$

• **An *F-Bar* implementation:** Basically, the *F-bar* methodology requires that the deformation gradient be decomposed into a volumetric and an isochoric component, i.e., $\mathbf{F} = \mathbf{F}_{dev}\mathbf{F}_{vol}$ with $\mathbf{F}_{dev} = [\det \mathbf{F}]^{-\frac{1}{3}} \mathbf{F}$ and $\mathbf{F}_{vol} = [\det \mathbf{F}]^{\frac{1}{3}} \mathbf{I}$. Moreover, in the *F-bar* methodology the $\mathbf{F}_{vol}$ is computed as a constant term inside the element. Here, one assumes:

$$\overline{\mathbf{F}} = \mathbf{F}_{iso}\left(\mathbf{F}_a\right)_{vol} = \left(\frac{\det \mathbf{F}_a}{\det \mathbf{F}}\right)^{\frac{1}{3}} \mathbf{F} \quad \text{with} \quad \det \mathbf{F}_a = \frac{1}{\Omega_e} \int_{\Omega_e} \det \mathbf{F}\, d\Omega_e \tag{21}$$

The derivation of the internal force in Eq.(16) and the tangent stiffness in Eq.(17) is obtained by making the following composition $\mathbf{P} = \mathbf{P} \circ \phi(\mathbf{F})$ with $\phi(\mathbf{F}) = \overline{\mathbf{F}}$. Thus,

$$[\overline{\mathbb{A}}]_{ijkl} = \frac{\partial P_{ij}}{\partial \overline{F}_{rs}} \frac{\partial \overline{F}_{rs}}{\partial F_{kl}}. \tag{22}$$

6. Examples

(1) A simple tension-compression hyperelastic deformation test A simple tension-compression analysis is carried out in order to illustrate the nonlinear constitutive relation among the rotated *Kirchoff* stress and the logarithmic deformation. Considering an one-dimensional model, as illustrated in Figure 4, it can be shown that $\overline{T}_{zz} = E \ln\left(\lambda_z\right)$ with $E = \dfrac{9\kappa\mu}{3\kappa + \mu}$.

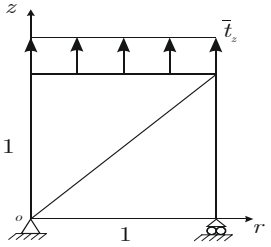

Fig. 4 One-dimensional axisymmetric model

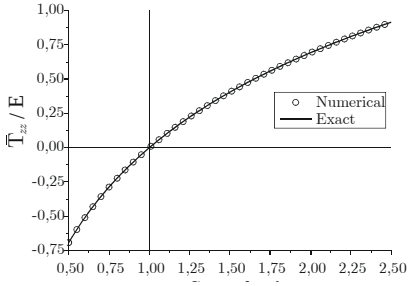

Fig. 5 Analytical x numerical results for simple tension-compression test

The material parameters adopted for this analysis are κ = 164206,35 MPa and μ = 80193,80 MPa. Figure 5 shows the analytical and the numerical comparison for this analysis in terms of the normalized stress ($\bar{T}_{zz}/E$) versus the stretch λ_z.

(2). Necking of a bar Here, we consider the analysis of an hypothetical cylindrical bar with the objective of verifying the necking behavior. The problem is illustrated in Figure 6. The model consists of a bar with a length of 53.334 mm and a radius of 6.413 mm. Due to the symmetry condition, only a quarter of the model is discretized. The model is submitted to a prescribed displacement of u_z=7 mm in the upper region of the bar. The prescribed displacement is applied by a linear ramp where several steps are considered. To trigger the necking, a small geometric imperfection is introduced in the model. This imperfection consists of a variation of the radius in the central region of 1%, i.e., the radius of the central region is 6.35 mm. Similar examples are presented in the works of Simo & Armero 0 and Souza Neto *et al.* 0 where an investigation of the volumetric locking problem was accomplished. Figure 6 shows the discretization of the domain into the triangular integration cells. Figure 6(a) presents a finite element mesh, employing classical tri6 finite elements, with 1379 nodes. Figures 6(b) and 6(c) show the MEFG particle distribution that contains 364 and 1379 nodes/particles, respectively. The material properties used are: κ = 164206,35 MPa, μ = 80193,80 MPa, H = 129.24MPa, δ =16.93, σ_∞ =715MPa and σ_y = 450MPa. Figure 7 shows the comparison among the deformed configurations of the body outline at 85% and 100% of the total prescribed displacement considering the meshes of Figure 6(a) and 6(c) with and without the *F-bar* methodology. Note that at 85% there is no apparent distinction between the two methods. However, at 100% of the process a discrepant difference is verified in the necking region. Note also that there is a relevant difference, in the necking region, when the *F-bar* methodology is considered.

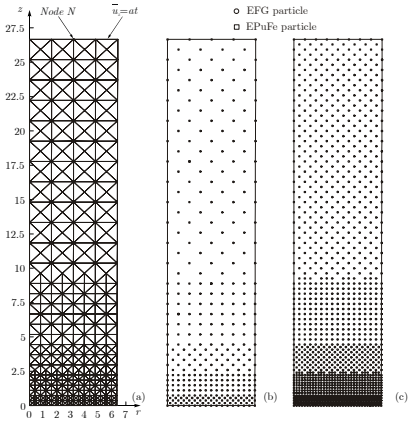

Fig. 6 Integration meshes a) FEM – 1379 nodes, b) MEFG – 364 nodes and c) MEFG – 1379 nodes

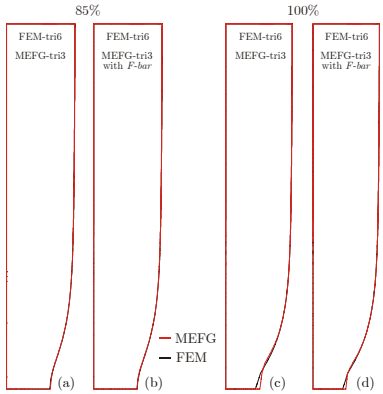

Fig. 7 Comparison among deformed bodies at 85% and 100% of the process.

Differences are also noted when the accumulated plastic strain analysis at a end of the process, shown in Figure 8, is considered. Again in this figure we consider the results for the meshes of Figure 6(a) and 6(c). Figure 9 plots the stress versus displacement diagram for the node *N*, see figure 6. It is clear from this figure that the results remain close to one another during a great part of the process. In a certain threshold point, looking what seems to be an inflection point, the solution moves away from that achieved by solving a finite element method. Notice again that the implementation of the *F-bar* procedure generate improved results when compared with the finite element solution.

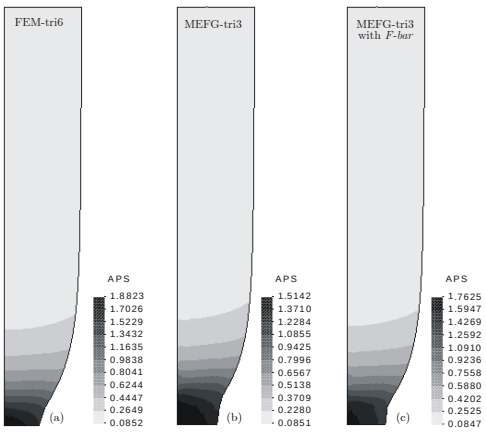

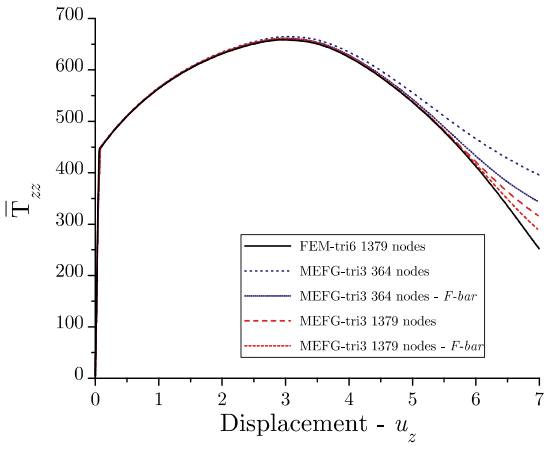

Fig. 8 Accumulated plastic strain at the end of the process.

Fig. 9 Comparison between stress x displacement, at node N, for the different methods and meshes.

7.Conclusions

In this work the modified element-free Galerkin method was numerically investigated under finite strains. Results shown in this paper evidence the presence of volumetric locking. Also it shows the improvement of the result once the *F-bar* approach is employed. Moreover, the results show that with an improved discretization of the domain, in the necking region, it is possible to reduce considerably the presence of volumetric locking. A possible reason for this behavior is the fact that the EPUFE global shape function, illustrated in Figure 2, interpolates **F(X)** as a constant and are employed in order to enforce the symmetry conditions. Thus, in this region, the *F-bar* is meaningless. The refinement of the mesh in the necking region reduced the effective area of the domain covered by the EPUFE global shape function. Thus,the implementation of a h-adaptive scheme may result in a volumetric lock free solution to the problem.

8. Acknowledgements

The support of the CNPq, Conselho Nacional de Desenvolvimento Científico e Tecnológico, of Brazil is gratefully acknowledged. Grant Number: 304020/2003-6

9. References

Huerta A., Méndez S. F., 2001, Locking in the incompressible limit for the element-free Galerkin method, Int. J. Numer. Meth. Engrg., 51, 1361-1383.

Eterovic A.L., Bathe K. J., 1990, A Hyperelastic-Based Large Strain Elasto-Plastic Constitutive Formulation with Combined Isotropic-Kinematic Hardening using the Logarithmic Stress and Strain Measures, Int. J. Num. Meth. Eng., 30, 1099-1114.

Akkaram S., Zabaras N., 2001, An updated Lagrangian finite element sensitivity analysis of large deformations using quadrilateral elements, Int. J. Num. Meth. Eng., 52, 1131-1163.

Souza Neto E. A., Peric D., Owen D. R. J., 2002, Computational Plasticity: Small and Large Strain Finite Element Analysis of Elastic and Inelastic Solids, Classroom Notes, University College of Swansea, Wales.

Souza Neto E. A., Peric D., Dutko M., Owen D. R. J., 1996, Design of simple low order finite elements for large strain analysis of nearly incompressible solids, Internat. J. Solids and Structures, 33, 3277-3296.

Weber G., Anand L., 1990, Finite deformation constitutive equations and a time integration procedure for isotropic, hyperelastic-viscoplastic solids, Comput. Methods Appl. Mech. Engrg. 79, 173-202.

Askes H., De Borst R., Heeres O., 1999, Conditions for locking-free elasto-plastic analyses in the Element-Free Galerkin method, Comput. Methods Appl. Mech. Engrg., 173, 99-109.

Simo J. C., Armero F., 1992, Geometrically Non-Linear Enhanced Strain Mixed Methods and the Method of Incompatible Modes, Int. J. Num. Meth. Eng., 33, 1413-1449.

Alves M. K., Rossi R., 2003, A modified element-free Galerkin method with essential boundary conditions, enforced by an extended partition of unity finite element weight function, Int. J. Num. Meth. Eng., 57, 1523-1552.

Ortiz M., Radovitzky R. A., Repeto E. A., 2001, The computation of exponential and logarithmic mappings and their first and second linearizations, Int. J. Numer. Meth. Engrg., 52, 1431-1441.

R. Hill, 1978, Aspects of invariance in solid mechanics, Adv. in Appl. Mech., vol. 18, pp. 1-75.

Belytschko T., Lu Y. Y., Gu L., 1994, Element-free Galerkin methods, Int. J. Numer. Meth. Engng. 37, 229-256.

Hughes T. J. R., 1980, Generalization of seletive integration procedures to anisotropic and nonlinear media, Int. J. Numer. Meth. Engrg., 15, 1413-1418.

Liu W. K., Li S., Belytschko T., 1997, Moving least-square reproducing kernel methods (I) Methodology and convergence, Comput. Methods Appl. Mech. Engrg. 147, 113-154.

Simo J. C., Rifai S., 1990, A Class of Mixed Assumed Strain Methods and the Method of Incompatible Modes, Int. J. Numer. Meth. Engrg., 29, 1595-1638.

Wells G. N., Sluys L. J., De Borst R., 2002, A *p*-adaptive scheme for overcoming volumetric locking during plastic flow, Comput. Methods Appl. Mech. Engrg., 191, 3153-3164.

Zabaras N., Ganapathysubramanian S., Li Q., 2003, A continuum sensitivity method for the design of multi-stage metal forming processes, Int. J. Mech. Sciences, 45, 325-358.

10. Responsibility notice

The authors are the only responsible for the printed material included in this paper.